Alpha Nickel Hydroxides as Lightweight Nickel Electrode Materials for Alkaline Rechargeable Cells

Wei-Kang Hu* and Dag Noréus

Department of Structural Chemistry, Arrhenius Laboratory, Stockholm University, S-106 91 Stockholm, Sweden

Received September 23, 2002. Revised Manuscript Received December 12, 2002

A lightweight nickel hydroxide electrode was obtained through developing a stable α-phase nickel hydroxide with a 10 at. % Al substitution. The effects of an Al addition within 10−30 at. % on the interslab distance of the (001) plane as well as on the electrochemical properties were investigated. Pasted α- and *β*-type nickel hydroxide electrodes were fabricated to compare the specific capacity, weight, and volumetric energy densities of both types of electrodes. The results showed the α-type nickel electrode to have a higher specific capacity and weight energy density than the *β*-type nickel electrode. The volumetric energy density of the α-type nickel electrode was, however, inferior to that of the *β*-type nickel electrode. Two type AA size NiMH cells were also constructed by spirally winding the α- and *β*-type nickel electrodes and AB_5-type MH electrodes, respectively. The cell performances were evaluated.

Introduction

Improvement of the nickel hydroxide powder in positive electrodes has become the highest priority for increasing the performance of rechargeable alkaline batteries. During the past decades, a pasted nickel electrode has been developed to replace conventional sintered nickel electrodes to improve the energy density of the nickel/metal hydride (NiMH) battery.[1−3] Compared with the sintered nickel electrode's energy density of 400−450 mA·h/cm^3, the pasted nickel electrode has a higher energy density reaching up to 550−620 mA·h/cm^3. The pasted nickel electrode can further be made at a low manufacturing cost with low emissions of waste materials. *β*-Phase spherical nickel hydroxide powders are usually used as active materials since the *β*-phase has a high tap density (2.1−2.2 g/cm^3) and good stability in an alkaline electrolyte. However, the *β*-phase nickel hydroxide has its theoretical capacity limit at 289 mA·h/g, which is almost reached in present batteries. Thus, the *β*-phase nickel hydroxide has limited possibilities for further improvement of the NiMH performance. In addition, the *β*-phase nickel hydroxide easily changes to *γ*-phase NiOOH when the electrode is overcharged. The formation of the *γ*-phase results in a swelling of the positive electrode volume by absorbing the electrolyte.[4] The redistribution of the electrolyte from the separator leads to a dry-out of the separator. As a result, the internal resistance in the cell rises with cycling, leading to deterioration and subsequent failure of the NiMH cells.

In recent years, α-phase nickel hydroxides have attracted much attention since the α-phase nickel hydroxide not only has a superior theoretical electrochemical capacity (433 mA·h/g with an average oxidation state of 3.5 or higher for nickel in the *γ*-phase[5−7]) but also exhibits no noticeable change of electrode volume when repeatedly charge−discharge cycled between the α- and *γ*-phase.[7−9] If the electrode swelling can be eliminated, many disadvantages in the current NiMH cells may be overcome. The pure α-phase nickel hydroxide is, however, very unstable in a strong alkaline medium and easily transforms to the *β*-phase after a few cycles.

Many studies by partial substitution of Co,[10−14] Fe,[15−17] Mn,[17−20] Al,[17,21−27] or Zn[28,29] for Ni were made

---

(1) Oshitani, M.; Yufu, H.; Takashima, K.; Tsuji, S.; Matsumaru, Y. *J. Electrochem. Soc.* **1989**, *136*, 1590.
(2) Oshitani, M.; Yufu, H. U.S. Patent, 4844999, 1989.
(3) Oshitani, M.; Watada, M.; Tanaka, T.; Iida, T. *Symposium on Hydrogen and Metal Hydride Batteries*, The Electrochemical Society Proceedings Florida, Oct 9−14, 1994; Vol. 94-27, pp 303−328.
(4) Oshitani, M.; Takayama, T.; Takashima, K.; Tsuji, S. *J. Appl. Electrochem*. **1986**, *16*, 403.
(5) Barnard, R.; Randell, C. F.; Tye, F. L. *J. Appl. Electrochem*. **1980**, *10*, 109.
(6) Corringan, D. A.; Knight, S. L. *J. Electrochem. Soc.* **1989**, *136*, 613.
(7) Faure, C.; Delmas, C.; Fouassier, M. *J. Power Sources* **1991**, *35*, 279.
(8) Bode, H.; Dehmelt, K.; Witte, J. *Electrochim. Acta* **1966**, *11*, 1079.
(9) Delmas, C.; Faure, C.; Borthomieu, Y. *Mater. Sci. Eng.* **1992**, *B13*, 89.
(10) Delmas, C.; Braconnier, J. J.; Borthomieu Y.; Hagenmuller, P. *Mater. Res. Bull*. **1987**, *22*, 741.
(11) Armstrong, R. D.; Charles, E. A. *J. Power Sources* **1989**, *25*, 89.
(12) Faure, C.; Delmas, C.; Fouassier, M.; Willmann, P. *J. Power Sources* **1991**, *35*, 249.
(13) Faure, C.; Delmas, C.; Fouassier, M.; Willmann, P. *J. Power Sources* **1991**, *35*, 263.
(14) Faure, C.; Delmas, C.; Fouassier, M.; Willmann, P. *J. Power Sources* **1991**, *36*, 497.
(15) Demourgues-Guerlou, L.; Braconnier J. J.; Delmas, C. *J. Solid State Chem*. **1993**, *104*, 359.
(16) Demourgues-Guerlou, L.; Delmas, C. *J. Power Sources* **1993**, *45*, 281.

10.1021/cm021312z CCC: $25.00

to stabilize the α-phase nickel hydroxide. According to these studies, the stability of α-phase nickel hydroxides in a strongly alkaline medium can be reached after a 20% substitution of nickel. The available capacity and energy density, however, usually decrease with increasing the percentage of substitution since the substitution element does not take part in electrochemical redox reaction. Therefore, it is desired that the substitution in the nickel hydroxide should be kept as low as possible. In this work, an attempt was made to investigate a lower Al substitution in the nickel hydroxide while remaining an α-phase structure. The effects of Al content on the interslab distance of the α-phase nickel hydroxide and electrochemical properties were also examined. The stabilized α-phase nickel hydroxide particle was then used as an active material of nickel electrodes. The weight and volumetric energy densities of the α-type nickel electrode were measured and compared with those of *β*-type nickel hydroxide electrodes. Two types of NiMH cells were constructed by spirally winding the α-type and *β*-type nickel electrodes respectively with the same type of metal hydride electrodes. The cell performances were evaluated.

Experimental Section

Sample Preparation and Characterization. The α-phase nickel hydroxide particles were prepared by adding a mixed solution containing $Ni(NO_3)_2{\cdot}6H_2O$ and $Al(NO)_3{\cdot}9H_2O$ in a required $[Ni^{2+}]/[Al^{3+}]$ ratio to a 0.5 M LiOH solution while stirring at 30 °C. The pH value of the solution after addition was about 7.0. Prior to filtering, the precipitate was aged in the mother solution for 24 h at 30−40 °C. The precipitate containing 10 at. % Al content was further treated at 100 °C for 72 h in the same mother solution. The precipitate was then washed with distilled water, filtered, and dried at 65 °C. The sample thus obtained was ground to a fine powder ($<36\ \mu m$) for X-ray diffraction (XRD) and electrochemical evaluations. To examine the stability of the 10 at. % Al substitution nickel hydroxide, one part of the sample was aged in 6 M KOH solution at room temperature. The other one was used as the active material of nickel electrode for electrochemical cycles in NiMH cells. Afterward, the phase structure of the sample after electrochemical cycles was further examined by XRD.

Evaluation of Electrochemical Properties. An α-type nickel hydroxide electrode was prepared by mixing an active powder (65.6 wt %) with Ni powder (Inco 210) (26.7 wt %), cobalt oxide powder (7.7 wt %), and carboxymethyl cellulose (CMC) as a binder on a nickel form substrate with a geometrical size of 2.0 × 2.0 cm at room temperature. The electrochemical properties were measured in a half-cell with a 6.0 M KOH solution at 22 °C. A metal hydride (MH) electrode with a capacity in excess of the nickel hydroxide electrode was uses as a counter electrode and a Hg/HgO (6.0 M KOH) electrode as a reference electrode. The nickel hydroxide electrode was charged at a rate of 0.3 C for 5 h and discharged at a 0.25 C rate to a cutoff potential of 0.1 V. The life-cycling measurement was carried out by charging at a rate of 1.0 C for 1.2 h and discharging at the same rate to an end potential of 0.1 V using a computer-controlled battery cycler. All potentials mentioned in this section are with respect to the reference electrode.

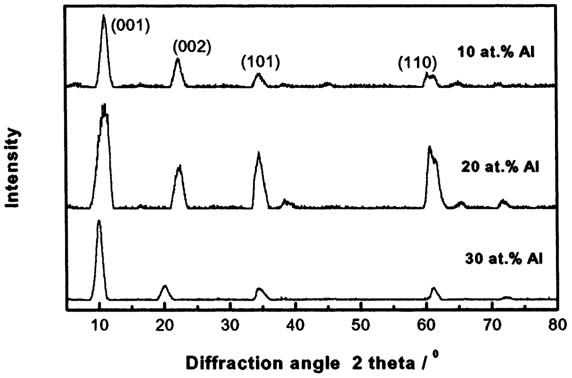

Figure 1. XRD patterns of α-phase nickel hydroxide powders.

Preparation of Pasted Nickel and MH Electrodes. In this section, the nickel hydroxide powder with 10 at. % Al content was used as active materials of α-type nickel electrodes. A pasted α-type nickel electrode was prepared as follows. The α-phase nickel hydroxide powder, Ni powder (Inco 210) and cobalt oxide powder, were mixed in a weight ratio of 79:14:7. A 1.0 wt % carboxymethyl cellulose (CMC) was added to the mixture to obtain a paste. A porous nickel foam with a dimension of 40-mm wide × 70-mm long × 1.6-mm thick was used as the nickel electrode substrate. The nickel substrate was then filled with the paste, dried, and mechanically pressed to 0.86-mm thick to obtain a commercial thickness α-type nickel electrode. For a metal hydride (MH) electrode, a standard AB_5-type hydrogen storage alloy with a capacity of 300−320 mA·h/g was used as the active material. The preparation process of the MH electrode is similar to that of the nickel electrode. The binding material for the MH electrode is poly(tetrafluoroethylene) (PTFE) solution. The MH electrode composition was fixed at 90.5 wt % MH alloy, 8.0 wt % Ni powder (Inco 210), and 1.5 wt % carbon powder. The final MH electrode size is 40-mm wide × 90-mm long × 0.35-mm thick.

NiMH Cell Assembly and Evaluation. A cylindrical AA size NiMH cell was assembled by spirally winding the nickel hydroxide positive electrode and the MH negative electrode along with a 0.01-mm-thick polyamide separator. The electrolyte used was 6.0 M KOH + 1.0 M LiOH. Before charge and discharge, the cell was placed in a thermostatic bath at 40 °C for 24 h. Then, the cell was charged and discharged at room temperature (22 °C) with a rate of 0.1 C for 15 h and the cutoff voltage was chosen to be 0.9 V for 2 cycles. Afterward, a 0.2 C rate charging for 6 h and discharging at the same rate were applied for long cycling time.

Results and Discussion

XRD Pattern and Character. Figure 1 shows the powder XRD patterns of the as-prepared nickel hydroxides with three different Al substitutions. The three samples all exhibit α-phase nickel hydroxide with a rhombohedral *P*3 structure. The chemical formula of the

---

(17) Indira, L.; Dixit, M.; Kamath, P. V. *J. Power Sources* **1994**, *52*, 93.

(18) Demourgues-Guerlou, L.; Delmas, C. *J. Power Sources* **1994**, *52*, 269.

(19) Demourgues-Guerlou, L.; Delmas, C. *J. Power Sources* **1994**, *52*, 275.

(20) Demourgues-Guerlou, L.; Delmas, C. *J. Electrochem. Soc.* **1996**, *143*, 561.

(21) Kamath, P. V.; Dixit, M.; Indira, L.; Shukla, A. K.; Kumar, V. G.; Munichandraiah, J. *Electrochem. Soc.* **1994**, *141*, 2956.

(22) Liu, B.; Wang, X. Y.; Yuan, H. T.; Zhang, Y. S.; Song, D. Y.; Zhou, Z. X. *J. Appl. Electrochem.* **1999**, *29*, 855.

(23) Buss, D. H.; Bauer, J.; Diembeck, W.; Glemser, O. *J. Chem. Soc., Chem. Commun.* **1985**, 81.

(24) Sugimoto, A.; Ishida, S.; Hanawa, K. *J. Electrochem. Soc.* **1999**, *146*, 1251.

(25) Ehlsissen, K. T.; Delahaye-Vidal, A.; Genin, P.; Figlarz, M.; Willmann, P. *J. Mater. Chem.* **1993**, *3*, 883.

(26) Dai, J.; Li, S. F. Y.; Xia, T. D.; Wang, D. M.; Reisner, D. E. *J. Power Sources* **2000**, *89*, 40.

(27) Caravaggio, G. A.; Detellier, C.; Wronski, Z. *J. Mater. Chem.* **2001**, *11*, 912.

(28) Dixit, M.; Kamath, P. V.; Gopalakrishnan, J. *J. Electrochem. Soc.* **1999**, *146*, 79.

(29) Tessier, C.; Demourgues-Guerlou, L.; Faure, C.; Basterreix, M.; Nabias, G.; Delmas, C. *Solid State Ionics* **2000**, *133*, 11.

Table 1. XRD Data for the α-Phase Nickel Hydroxide Powders with Different Al Contents

Al content	*hkl*	*d* (Å)	*hkl*	*d* (Å)
10 at. %	001	8.035	101	2.580
	002	3.997	110	1.536
20 at. %	001	8.091	101	2.596
	002	4.004	110	1.526
30 at. %	001	8.897	101	2.603
	002	4.434	110	1.516

α-phase nickel hydroxide is generally written as follows,[25]

$$\underbrace{[Ni_{1-x}M^{III}_{x}(OH)_2]^{x+}}_{\text{Slab}} \cdot \underbrace{[A^{-}_{y}B^{2-}_{z}\,mH_2O]^{x-}}_{\text{Interslab space}}$$

where M is trivalent metallic ions, A and B can be mono- and divalent anions, respectively, and $x = y + 2z$. The stability is attributed to the strongly electrostatic interaction between opposite charged layers in the structure. The water molecules are located in the negatively charged anion layer. The precipitation process of the α-phase nickel hydroxide in this work was conducted in an air atmosphere. A small amount of carbonate ion inevitably enters into the mother solution. Thus, the anions inserted within the interslab could contain both nitrate and carbonate ions. The interslab distance of the α-phase nickel hydroxide varies depending on the amount and size of the inserted anions and on the number of incorporated water molecules. In our case, the prominent $d_{(001)}$ distance in the three α-phase nickel hydroxides varies between 8.0 and 8.9 Å, as seen in Table 1. The interslab distance increases with increasing Al content. An explanation was suggested as follows. The amount of positive charge in the composition of $[Ni_{1-x}Al_x(OH)_2]^{x+}$ increases with increasing Al content. To compensate for the excess of positive charge, the interslab region needs more anions. Thus, the increase of Al content in the samples results in an increase in the spacing of the (001) plane. This increase subsequently enlarges the unit cell volume and lowers the tap density (the tap density decreases from 1.2 to 1.0 g/cm^3 as the Al content increases from 10 to 30 at. %). This means that a high Al substitution will not be beneficial for reaching a high energy density. Since the energy density of an electrode is a key parameter for practical NiMH cells, the Al substitution must be kept at a minimum. In our experiments, the sample containing as low as 10 at. % Al still had sufficient stability. No β-phase structure was observed, even after the sample was left in 6.0 M KOH for 48 days at room temperature.

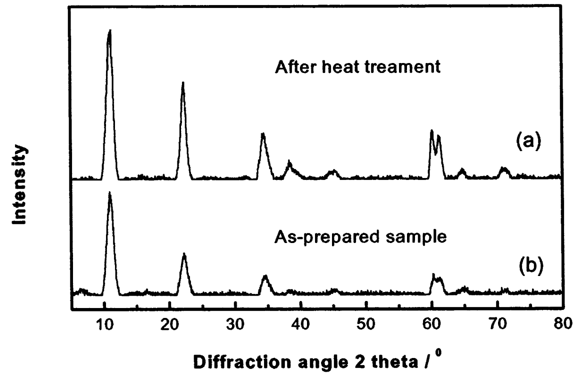

Figure 2. XRD pattern of the α-phase nickel hydroxide powder with 10 at. % Al after heat treatment of the as-prepared sample.

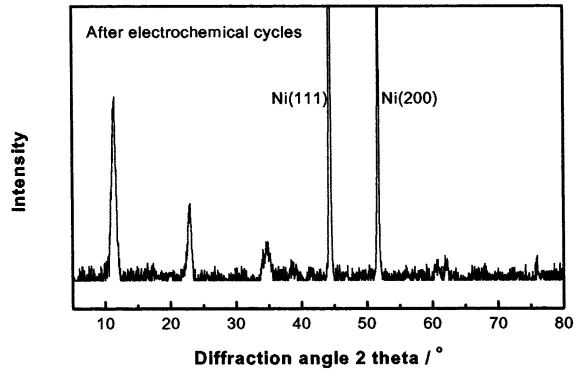

Figure 3. XRD pattern of the α-phase nickel hydroxide powder with 10 at. % Al after electrochemical cycles.

Figure 2 shows the XRD patterns of the sample after heat treatment at 100 °C for 72 h. After the heat treatment, some diffraction peaks at 37°, 47°, and ca. 71° can be seen and the peak at some 60° was more clearly split into two. Those peaks are still indexed in the α-phase structure. In addition, the diffraction peaks of the (001) and (002) planes become sharp compared with those of the as-prepared sample. These results indicated that the sample crystallinity was improved by the heat treatment. Figure 3 shows the XRD pattern of the 10 at. % Al-substituted sample after 300 charge−discharge cycles in the NiMH cells. As can be seen, the nickel hydroxide remains in an α-phase structure and no β-phase peaks were detected. These results show that the sample containing 10 at. % Al still had good chemical and electrochemical stability, even after aging in strongly alkaline solution or electrochemical cycles in the NiMH cells. The good stability of the α-phase nickel hydroxide with 10 at. % Al substitution could be attributed to a low pH value applied during precipitation. A lower pH value during preparation leads to hydroxide vacancies in the hydroxide layer.[25] To compensate for the hydroxide vacancies, more nitrate ions are needed in the interslab region, leading to better stability. Thus, a chemical formula of the stabile α-phase nickel hydroxide is proposed as follows:

$$\underbrace{[Ni_{1-x}Al_{x}(OH)_{2-(y-x)}]^{y+}}_{\text{Slab}} \cdot \underbrace{[(NO^{-}_{3})_{y}\,(mH_2O)]}_{\text{Interslab}}{}^{y-}$$

Electrochemical Properties. Figure 4 shows the discharge curves of the three as-prepared α-type nickel hydroxide electrodes after activation. It was found that the electrochemical capacity decreases with increasing Al content, namely, 320 mA·h/g for the electrode containing 10 at. % Al, 300 mA·h/g for the electrode containing 20 at. % Al, and 284 mA·h/g for the electrode containing 30 at. % Al. The drop of the specific discharge capacity is associated with the percentage of aluminum substitution since it does not take part in electrochemical redox reactions. In addition, it was observed that the average discharge potential increases with increasing Al content as shown in Figure 4. The reason for this

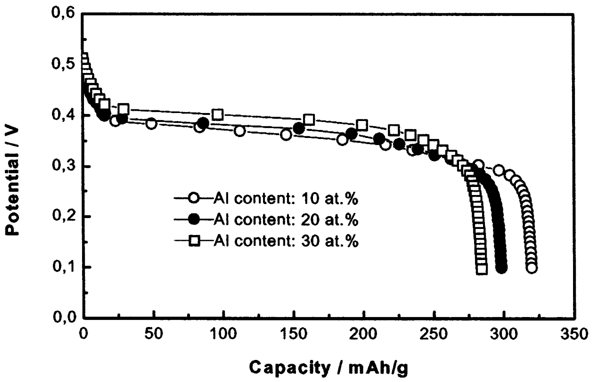

Figure 4. Discharge curves of the α-phase nickel hydroxide electrodes.

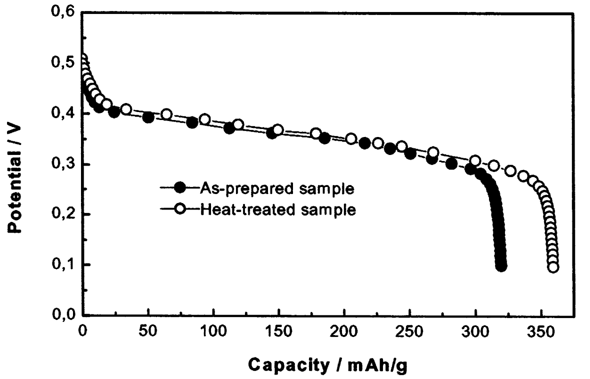

Figure 5. Comparison of discharge curves between two α-phase nickel hydroxide electrodes.

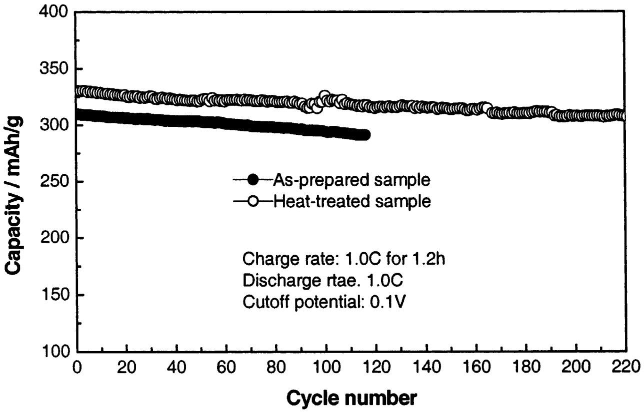

Figure 6. Comparison of cycling stability between two α-phase nickel hydroxide electrodes.

effect is probably related to the *d* spacing of the (001) plane and the amount of intercalated anions. A wider interlayer spacing with more intercalated water molecules might facilitate the diffusion of hydrogen during the discharging. Figure 5 shows the discharge curves of the as-prepared and the heat-treated samples with a 10 at. % Al content. The heat-treated sample exhibits a higher discharge capacity than the as-prepared sample. The cycling stability of the heat-treated sample also seems to be better, as shown in Figure 6. The reason the heat-treated sample has a better electrochemical performance could be attributed to the better crystallinity. A similar phenomena has also been observed by other authors.[24]

Electrode and Cell Performances. The discharge curves of the negative MH and positive nickel electrodes are shown in Figures 7 and 8, respectively. For comparison, a *β*-type nickel hydroxide electrode is also presented in Figure 8. The negative MH alloy has a specific capacity of 310 mA·h/g and the energy density of the electrode reaches about 1430−1450 mA·h/cm^3. As seen from Figure 8, the specific capacities of the α- and *β*-phase nickel hydroxides are about 350 and 273 mA·h/g, respectively. The former has a higher specific capacity than the latter. This implies that a lightweight nickel electrode could be made by using the α-phase nickel hydroxide. At the moment, the weight energy densities of the α- and *β*-type nickel electrodes are about 217 and 180 mA·h/g, respectively, which includes the weight of the electrode substrate. But the α-type nickel electrode has a relatively lower volumetric energy density compared with the *β*-type nickel electrode. The volumetric energy densities of the α- and *β*-type nickel electrodes are some 500 and 620 mA·h/cm^3, respectively, in this work. Figure 9 gives the electrochemical performance of two type AA size NiMH cells. The cell containing a *β*-type nickel electrode has a capacity of 1500 mA·h at a 0.2 C rate. However, a further improvement in this cell capacity is severely limited since the utilization of the *β*-type nickel electrode is already close to the theoretical maximum.

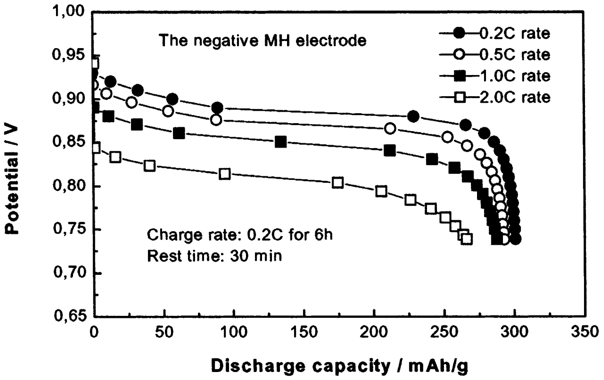

Figure 7. Discharge curve of the negative MH electrode.

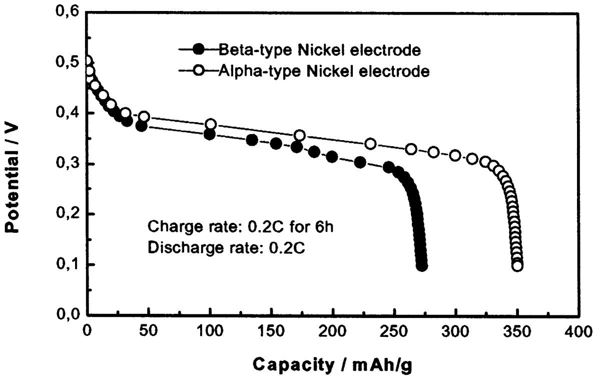

Figure 8. Discharge curves of the α- and *β*-type nickel hydroxide electrodes.

The cell made with an α-type nickel electrode had a lower capacity compared to the cell containing a *β*-type nickel electrode. This is because less α-type active material can be filled into a nickel substrate of the same dimension as for the *β*-type nickel electrode. In this work, only 3.2 g of α-type active material could be filled into the AA size positive electrode due to its lower tap density (about 1.2 g/cm^3). In contrast, about 5.5 g of *β*-phase active materials could be used for the same size

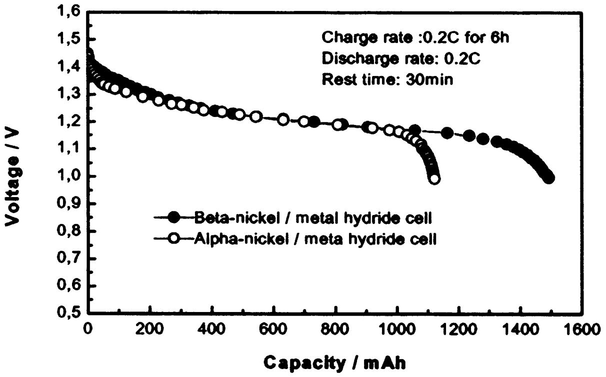

Figure 9. Comparison of discharge performance of the α- and β-type nickel/metal hydride cells.

electrode. If the tap density of the α-phase nickel hydroxide could be improved by a modest 20% and its capacity reaches 380−420 mA•h/g,[24,30] an AA size α-type cell would reach a capacity beyond 1500 mA•h. If these assumptions are verified soon, the weight and volumetric energy densities of the α-type nickel electrode will increase to >225 mA•h/g and >630 mA•h/cm^3, respectively.

Anyhow, a lightweight nickel electrode for alkaline rechargeable cells or Ni−H_2 cells could be obtained by using α-phase nickel hydroxide materials. It is particularly important for Ni−H_2 cell applications in aerospace and spacecraft power systems since the weight is a key parameter. Moreover, there are many opportunities for further improvement in the weight and volumetric energy densities of the α-type nickel electrode through improving the preparation process and synthetic conditions of the α-phase nickel hydroxide particles since the current capacity available and tap density of the α-phase nickel hydroxide particle are far below the theoretical values of 433 mA•h/g and 2.82 g/cm^3. Hence, the α-type nickel electrode has a good potential for increasing its specific capacity and energy density.

Conclusion

α-Phase nickel hydroxide powders with 10−30 at. % Al contents were prepared by chemical precipitation. The XRD examinations showed that the interslab distance between two hydroxide layers increased with increasing Al content. The electrochemical discharge capacity decreased as the Al content increased. It was found that an α-phase nickel hydroxide with a 10 at. % Al content had satisfactory stability in a strong alkaline medium (6.0 M KOH). No β-phase nickel hydroxide was detected after being aged in 6.0 M KOH for 48 days at room temperature or after electrochemical cycling for 300 cycles in the NiMH cells. The sample crystallinity could be improved by heat treatment, resulting in further improvement of electrochemical capacity and cycling stability.

Metal hydride electrodes and α-type nickel hydroxide electrodes with commercial thickness were also fabricated to make an AA size α-type NiMH cell. For comparison, an AA size β-type NiMH cell was also assembled. The results show the α-type nickel electrode has a higher specific capacity and weight energy density. The α-phase nickel hydroxide still has substantial possibilities for further improvements in the weight and volumetric energy density.

CM021312Z

---

(30) Chen, H.; Wang, J. M.; Pan, T.; Xiao, H. M.; Zhang, J. Q.; Cao, C. N. *Int. J. Hydrogen Energy* **2002**, *27*, 489.